

Verification of dipole fit source localization in patients with epilepsy using postoperative MRI

Gülsüm Akdeniz

Department of Biophysics, Medicine Faculty, Yıldırım Beyazıt University; and Yenimahalle Training and Research Hospital, Ankara, Turkey

Abstract

Objective: Dipole fit source (DFS) localisation is a non-invasive imaging process used to identify the epileptogenic zone (EZ) in the brain. The purpose of the present study was to verify the use of DFS localisation for identifying the EZ in patients with and without lesions using magnetic resonance imaging (MRI). **Methods:** In this study, DFS localisation was used in 16 patients, of whom 7 had no lesions and 9 had lesions on MRI post-surgery, with at least 3 years of follow-up data. For DFS localisation, different scalp electroencephalogram (EEG) ictal activity was assessed (ictal spikes, rhythmic, paroxysmal fast, and obscured activity). DFSs were superimposed with postoperative MRIs to confirm the accuracy of the determined EZs. **Results:** The DFS correctly identified EZ localization within the resection area in 14 of the 16 patients. These 14 patients were all seizure free after surgery. The two remaining patients, in whom the DFS was adjacent to the resected area, had a decreased seizure frequency following surgery.

Conclusions: DFSs determined during preoperative evaluations can provide information on EZ lateralisation and localisation and contribute to the presurgical decision process. Thus, the accurate identification of EZ boundaries is important and can be achieved more reliably with the use of multiple quantitative EEG analysis methods.

Keywords: Epileptogenic zone, EEG source imaging, presurgical evaluation, epilepsy surgery, ictal spikes.

INTRODUCTION

Electrical source localization (ESL) is a non-invasive imaging method that can be used to identify the epileptogenic zone (EZ) in the brain. In ESL, two main approaches have been proposed by researchers; dipole and distributed source localization.¹ Dipolar models have been poorly investigated compared to the distributed source localization models. Distributed models include LORETA^{2,3} and sLORETA⁴ which are reliable methods to locate the EZ.

The dipole fit source (DFS) method is one of the main models used to estimate the location of a small number of focal sources. It models the neural sources as one or a few current dipoles using mathematical procedures.⁵ In DFS modelling, the key constraints are the type and the number of dipoles selected a priori for ESL.⁶ The modelling current dipole is the best fit for the spatial potential distribution and temporal variation of the measured epileptic spike for the location and orientation of the dipole.⁷ However, the

DFS is limited to visualize the three-dimensional space within the brain, and this limitation can be overcome by magnetic resonance imaging (MRI). Therefore, electroencephalography-magnetic resonance imaging (EEG-MRI), called electrical source localization (ESL), gives more accurate and reliable information about the EZ in the brain.

In the early 1990s, research efforts were made to investigate the benefits of the DFS method to evaluate candidates for epilepsy surgery.⁸⁻¹¹ Recent studies have demonstrated the ability of DFS localization to detect the EZ using interictal epileptiform discharges.¹²⁻¹⁴ Several studies have employed the DFS to determine the EZ in temporal lobe epilepsy patients with and without lesions on MRI.^{12,15-17} Although the pathologies of the patients differed, including focal cortical dysplasia (FCD), hippocampal sclerosis, and ganglioglioma, we conducted ESL using the DFS technique. The utilisation and advantages of the DFS technique in epilepsy surgery were investigated. Most studies concluded that the orientation of the

dipole was essential for proper interpretation of source solutions.¹⁸⁻²³ However, these studies are insufficient to demonstrate the clinical utility and cost-effectiveness¹⁴ in presurgical investigations of patients with focal epilepsy.

In the present work, ESL was performed using the DFS to estimate the EZ from scalp EEG ictal activity. The main aim of this study is to assess correlation of the EZ revealed by DFS localization and the postoperative MRI of patients with the outcome.

METHODS

Patients and EEG recording

In this retrospective study, we evaluated 16 multi-drug resistant focal epilepsy patients who had undergone electrical source localization and operated on with a post-operative follow-up for at least 3 years. The demographic and clinical data of the 16 patients included in the study are summarized in Table 1.

All patients had undergone extensive presurgical evaluation including Video EEG Monitoring (VEM) and proper MRI with epilepsy protocol. At the post-operative second month MRI scan was performed to all patients. The age range of the patients was 14-49 years (five females, mean age 27, median age 26 years). There were 12 temporal lobe epilepsy (TLE) patients and four extra-temporal lobe epilepsy (ETLE) patients.

High-resolution EEG data for all patients were recorded using long-term video EEG recording with 64 scalp electrodes (SynAmps; Compumedics Neuroscan, Charlotte, NC, USA, or SD LTM64 Headbox; Micromed, Italy). Electrodes were placed according to the 10-20 montage international system. Impedances were < 5 k Ω , and the signal was sampled at 256 Hz and digitized. The stored data were filtered off-line using 0.5-100 Hz band-pass digital filters.

Approval for the study was obtained from the Cerrahpaşa Medical Faculty Ethics Committee of Istanbul University (B-29).

Scalp ictal EEG quantitative analysis

Selection, detection, and analysis of the scalp EEG ictal patterns were performed using the Advanced Signal Analysis (ASA) software (ANT Software, Enschede, the Netherlands). For DFS analysis, the seizures were separated into individual events. Ictal activities on scalp EEG were used and classified according to Foldvary *et al.*²⁴ as ictal spikes, rhythmic, paroxysmal fast,

and obscured activity.

EEG time segments (epochs) of 250 ms around the spike's maximal peak were selected for DFS analysis. Ictal spikes were selected for dipole analysis by visual inspection of the EEG recordings. In this analysis, single moving dipole approach was used where one solution is calculated for each sampling point. Dipole positions, orientations and strengths were calculated separately for every time point resulting in a trace of dipoles with the single moving dipole model. This method allows to determine if we can identify a particular area as the origin of the activity when the localization of the equivalent current dipole remains stable in the same area for sufficient time (20-30 ms). DFS modeling was created by analyzing 15-20 ictal activities per seizure via ASA software.

Localization of the electrode position and MRI

In all patients, all EEG electrodes were localised using the fiducial system, defined by anatomical landmarks (nasion, right and left tragi), registered labelling of EEG sensors and automatic localization in the MRI volume.

According to a standardized epilepsy protocol, post-surgical evaluation using high-resolution 1.5 T scanners was used to obtain MRI (Magnetom Avanto, Siemens, Erlangen, Germany) scans from all patients. The MRI protocol consisted of a fat-suppressed non-contrast-enhanced T1-weighted sequence (repetition time/echo time [TR/TE] = 545/8 ms; receiver bandwidth = 22 kHz; section thickness = 6 mm; interslice gap = 0.5 mm; matrix size = 320 × 216; field of view [FOV] = 400 mm × 400 mm; scan time = 2 minutes) and a T2-weighted sequence (TR/TE = 3400/100 ms; receiver bandwidth = 20 kHz; section thickness = 4 mm; interslice gap = 0.5 mm; matrix size = 320 × 240; FOV = 250 mm × 250 mm; scan time = 2 minutes 52 seconds).

Individual head model

To create individual head models using three-dimensional patient's MRI, we identified the same three points (nasion, right and left tragi). Identification of the same spatial reference for neurophysiological and structural data was performed. The individual head model was based on the boundary element method, which consists of three compartment surfaces (brain, skull, and scalp) and is described by triangulation using 4000 nodes per model. An individual EEG matrix was calculated using ASA software. Each compartment

of specific conductivity was attributed to each volume (brain = 0.33, skull = 0.0042, and scalp of each patient = 0.33 Siemens/meter).

Dipole fit source (DFS) model

In the DFS model, a single dipole was used to model the voltage field at any instance giving the best fit. Each consecutive field measurement was constructed using different single dipoles. Over time, the term “moving dipole model” led to the dipole solution, which involves changes in location and orientation.²⁵⁻²⁸ This source modelling method depends on the hypothesis stating that the cortical sources of the spike or seizure potentials at each instant can be constructed adequately as a single dipole, and that consecutive single dipoles over time can sufficiently examine the movement of the source, i.e., propagation.

Dipolarity is a goodness-of-fit of the dipole approximation, and the reliability of the dipole fit method was evaluated by goodness of fit (GOF).⁶ GOF calculated using ASA software after MRI co-registration. DFSs were identified in postoperative MRIs were then compared with localizations obtained by DFS model. DFS images with two sets of reference standards (gold standards) were compared. For each patient, DFS images were compared with the resected areas and the surgical outcome three year after the operation.

RESULTS

ESL was performed in 16 patients, of whom 7 were MRI negative and 9 had lesions on MRI. The anatomical information obtained from the DFS is shown in Table 2.

Patient groups according to scalp EEG ictal activity

DFS localization was classified according to ictal activity on scalp EEG consisting of ictal spike activity for five patients, rhythmic activity for five patients, paroxysmal fast activity for four patients and obscured activity for two patients. The scalp EEG ictal activity showed ictal spike activity in three MRI negative patients (P12, P14 and P15) and two patients (P1 and P6) with lesions on MRI, rhythmic activity in MRI negative three patients (P5, P13 and P16) and two patients (P2 and P3) with lesions on MRI, paroxysmal fast activity in one MRI negative patient (P10) and three patients with lesions on MRI (P4, P7 and P8), and obscured activity in two patients (P9 and P11) with lesions on MRI (Table 1).

Dipole fit source (DFS results) for patients with temporal lobe epilepsy (TLE) and extra-temporal lobe epilepsy (ETLE)

ESL was performed in 12 patients with TLE, of whom 3 were MRI negative and 9 had lesions on MRI. Eight patients had right TLE and four had left TLE (Table 1). ESL was performed in four patients with ETLE. All of them were lateralized to left and MRI negative (Table 1).

Verifying dipole fit source (DFS) data and resection zone localization

Verifiable data between the source localization methods and the patient’s postoperative MRI data (Figure 1) was obtained by DFS modelling. The DFS model was verified if both results indicated the same location in the same lobe, if the single dipole was adjacent to operated area or far away from it the DFS model was considered as unverified.

DFS correctly identified the EZ within the resected area in 11 of 12 patients with TLE and 3 of 4 patients with ETLE. In one patient with ETLE and one with TLE, the EZ was located adjacent to the resected area according to DFS (Figure 1).

Histopathology and postoperative outcome

In seven MRI negative patients, six (P12, P13, P15, P10, P14 and P16) had focal cortical dysplasia (FCD) and one (P5) had both FCD and hippocampal sclerosis on histopathological examinations. MRI revealed structural lesions in nine patients: three (P6, P8 and P11) with hippocampal sclerosis, two (P3 and P2) with both FCD and hippocampal sclerosis, one (P7) with FCD, one (P4) with ganglioglioma, one (P1) with pleomorphic xanthoastrocytoma and one (P9) with neurofibromatosis. Of the 16 patients, 14 were seizure-free after surgery. The remaining two patients (P15 and P16) had a decreased number of seizures post-surgery.

DISCUSSION

Successful epilepsy surgery is improved by precise and accurate identification of the EZ. Despite improvements in medical imaging techniques, there are still disagreements on which technique is the most appropriate. In this study, the EZ was detected by using the DFS technique, which utilizes data from non-invasive EEG recording. The EZ was determined using distinct types of scalp EEG activities and assessed by superposition

Table 1: The demographic, EEG localization, MRI, FDG-PET operation region, pathology result, follow-up time after surgery, and seizure outcome data of the 16 patients included in the study

Patient	Gender/ Age	Ictal EEG Localization	MRI	PET	Operation Side	Pathology	Postoperative Follow-up Time	Postoperative Seizure Condition
P1	M/19	Left temporal	In right fusiform gyrus and parahippocampal gyrus, cortical organization disorder	Right mesial temporal hypometabolism	Right fusiform gyrus and inferior temporal gyrus	Pleomorphic xanthoastrocytoma	59 months	Absent
P2	F/30	Right mesial temporal	Right temporal cortical organization disorder	Right temporal lateral + mesial hypometabolism	Right Temporal	Right mesial temporal sclerosis + FCD	56 months	Absent
P3	M/24	Right mesial temporal	Right mesial temporal sclerosis	At the level of the pole, distinct right temporal lateral + mesial hypometabolism	Right mesial Temporal	Hippocampal sclerosis + middle, inferior, superior, temporal gyri, FCD Type I	48 months	Absent
P4	F/21	Right temporal	Along the right fusiform gyrus and parahippocampal gyrus, thicker cortex than normal + right hippocampal sclerosis	Right mesial temporal hypometabolism	Right temporal	Ganglioglioma	63 months	Absent
P5	M/35	Right mesial temporal	Normal	Normal	Right temporal	inferior, temporal + In fusiform gyrus FCD Type I + hippocampal sclerosis	66 months	Absent
P6	M/22	Right mesial temporal	Right mesial temporal	Right temporal mesial and lateral hypometabolism	Right temporal	Hippocampal sclerosis Type I	68 months	Absent
P7	M/27	Right occipital	Right temporo- occipital lobe lesion	Right temporo- occipital lobe hypometabolism	Right temporal	FCD Type II	64 months	Absent

Patient	Gender/ Age	Ictal EEG Localization	MRI	PET	Operation Side	Pathology	Postoperative Follow-up Time	Postoperative Seizure Condition
P8	M/25	Left mesial temporal	Left anterior temporal signal increasing	Left temporal hypometabolism	Left Temporal	Hippocampal sclerosis Type I	62 months	Absent
P9	M/34	Left temporal	Loss of cortical subcortical volume; left temporo-central/inferior temporal gyri all occipital lobe; parietal lobe posterior	Left temporo-occipito-parietal hypometabolism	Left inferior temporal gyrus + lateral temporo-occipital gyrus	Neurofibromatosis	43 months	Absent
P10	M/28	Left frontotemporal	Normal	Left temporal lobe hypometabolism	Left temporal	FCD Type II	50 months	Absent
P11	F/42	Left temporal	Left mesial temporal sclerosis	Left temporal lobe hypometabolism	Left temporal	Hippocampal sclerosis	69 months	Absent
P12	M/25	Left frontal cingulate or orbitofrontal	Normal	Normal	Left frontal	FCD Type I	47 months	Absent
P13	M/21	Left parieto-occipital	Normal	Left inferior temporal lobe hypometabolism	Left parietal	FCD Type I	46 months	Absent
P14	F/14	Left temporo-central	Normal	Normal	Left precentral/postcentral gyri + superior temporal gyrus, supramarginal gyrus	FCD Type II	38 months	Absent
P15	F/30	Left temporo-occipital	Normal	Normal	Left inferior parietal lobe + precuneus	FCD Type I	41 months	Decreased
P16	M/49	Right temporal	Normal	In right frontobasal and frontoanterior sections, hypometabolism	Right superior middle temporal gyrus + angular gyrus	FCD Type II	67 months	Decreased

P: Patient, M: Male, F: Female, FCD: Focal cortical dysplasia

Table 2: DFS localization results and summarized epileptogenic zone for each patients.

Patient	Dipole Fit	GOF (%)	Patient	Dipole Fit	GOF (%)
P1	Right mesial temporal	81.3	P9	Left mesial temporal	79.3
P2	Right temporal	57.1	P10	Left inferior temporal gyrus	83
P3	Right temporal pole	89.7	P11	Left temporal	75.6
P4	Right temporal pole	64.4	P12	Left superior frontal gyrus mesial face inferior	82
P5	Right temporal	52.0	P13	Left supramarginal gyrus superior	81
P6	Right mesial temporal	66.4	P14	Left precentral gyrus distal 1/3	66.7
P7	Right inferior temporal	72.5	P15	Left postcentral gyrus	62.6
P8	Left mesial temporal	70.6	P16	Mesial temporal gyrus	52.4

*GOF: Goodness of Fit

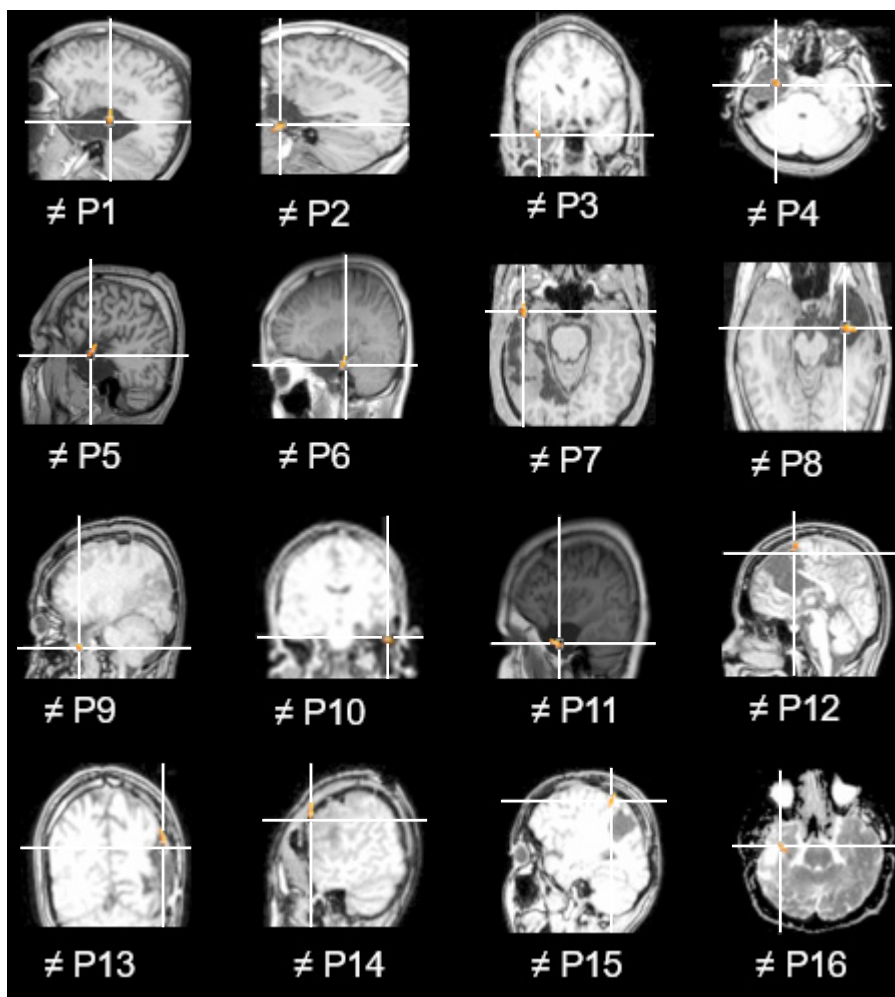


Figure 1. Results of DFS localisation superimposed on individual postoperative MRI for each patient. The resection areas are shaded in black, and a single dipole is shown in orange. We were able to predict the epileptic focus within the resected area in 14 of 16 patients.

between the resected area and DFS results. By co-registering the DFS results with the postoperative MRI scans, a 87.5% consistency was evident.

The primary reason for choosing DFS localization over other ESL methods is that the dipole location identifies only the “centre of mass” of the cortical source and not its extent or the specific cortex in the region. Because this point source model is used to explain the scalp field resulting from an extended source, the dipole model is typically located deep in the actual source cortex. The location of the epileptogenic DFS is determined by a single dipole, which involves a small area. However, the resected brain zone involves a greater area. Thus, detection of the area surrounding the dipole and the actual diameter will give a more reliable preoperative evaluation. In the dipole model, the average dipole orientation time was determined from the pre-seizure period. Depending on the seizure period, the dipole may differ in direction and orientation.^{7,29} Therefore, it might be useful to consider multiple signal classification (MUSIC) findings to determine the actual diameter of the dipole. Both the MUSIC and DFS methods provide consistent information, which is used to calculate an accurate EZ.

The correct localization can be achieved for all types of scalp EEG patterns.^{3,4} In that study, the different ictal activities (ictal spike, rhythmic, paroxysmal fast, and obscured activities) were used for analysis. Scalp EEG recordings were compared with postoperative MRI findings in 14 patients, and accurate EZ was determined and verified by previous study findings.^{17,30-32} In our study the DFS in two patients (P15 and P16, with decreased seizures post-surgery) was estimated near the resected area but was not as well localised. This finding suggests that the estimated zone might be involved in the EZ hence the patients did not become seizure free.

In a study of 20 patients with lesional temporal lobe epilepsy 64 channelled EEG records, real head model and dipole adaptation algorithms to measure the intracranial spike and slow activity for ESL analysis were used. An intracranial recording was obtained using three different areas: lateral (L), medial (M) and media-lateral (ML). In the L group (three patients), the interictal spike waves in the surface EEG were recorded as high signal noise. The interictal spread and source location were detected either partly or completely. In the M group (six patients), the spike activity was rarely seen in four patients, and none of these activities were localised. The authors indicated that the correct source localization can be achieved

only in the lateral part of the temporal lobe.¹⁷ In our study, the correct ESL was performed using DFS in nine patients with lesional TLE. Although Gavaret *et al.* performed ESL using a real head model, they analysed interictal EEG data. Our findings suggest that analysing ictal EEG data and using the real head model provide an accurate ESL for TLE in the medial group, which differed from the findings of Gavaret *et al.*

Gavaret *et al.* performed ESL by analysing interictal spike wave activity in 10 patients (of whom three were MRI negative) with frontal lobe epilepsy.³¹ They used 64 channel EEG recordings for ESL, a real head model and DFS algorithms. They evaluated lateral, medial and basal groups to determine the location of the interictal spike wave. In the lateral and medial groups, source localization was achieved by analysing interictal spike wave activity. The authors concluded that frontal lobe epilepsy can be detected by analysing ictal spike activity for highly accurate source localisation.³¹ In our study, we performed source localization and dipole adaptation using a real head model in one MRI negative patient with frontal lobe epilepsy (P12), which detected the ictal spike activity. The reliability of ESL, which was conducted using the DFS technique, was calculated, and the GOF was determined to be 82%. When these numerical results were demonstrated using a statistical mapping technique, we found the area overlapped the resected brain zone. This finding is in agreement with other findings.³² However, further studies involving a greater number of frontal lobe epilepsy patients are needed.

In the last decade, studies demonstrating that the localization provided by spike dipole modelling correlated well with other localization tools, such as intracranial EEG^{33,34}, PET³⁵, single photon emission tomography^{35,36}, and MRI³⁷, in both adults and paediatric patients.³⁸ The originality of this study is the comparison of postoperative MRI and DFS results in 16 patients who underwent epilepsy surgery and had been followed up at least for 38 months.

The DFS technique supported by MUSIC and mixed methods is extra informative for detecting the brain areas responsible for seizures in patients who are candidates for epileptic surgery. This study revealed that DFS can be utilised for presurgical evaluation of epilepsy. DFS may help to make a hypothesis on seizure onset zone and could be useful in planning of Stereo EEG electrode implantation.

ACKNOWLEDGMENTS

I am thankful to advisor of my thesis Professor Çiğdem Özkara, my co-supervisor Professor Mustafa Uzan and Professor Pekcan Ungan for providing discussions in every phases of this study.

DISCLOSURE

Financial support: The present work was supported by the Research Fund of Istanbul University. Project No: 19321.

Conflict of interest: None

REFERENCES

1. Michel CM, Murray MM, Lantz G, *et al.* EEG Source Imaging. *Clin Neurophysiol* 2004; 115:2195-222.
2. Pascual-Marqui RD, Michel CM, Lehmann D. Low resolution electromagnetic tomography: a new method for localizing electrical activity in the brain. *Int J Psychophysiol* 1994; 18:49-65.
3. Akdeniz G. Electrical source localization by LORETA in patients with epilepsy: Confirmation by postoperative MRI 2016; 19(1):37-43.
4. Koessler L, Benar C, Maillard L, *et al.* Source localization of ictal epileptic activity investigated by high resolution EEG and validated by SEEG. *NeuroImage* 2010; 51(2):642-53.
5. Cuffin BN. EEG dipole source localization. *IEEE Engineering in Medicine and Biology* 1998; 118-122.
6. Fuchs M, Wagner M, Kastner J. Confidence limits of dipole source reconstruction results. *Clin Neurophysiol* 2004; 115:1442-51.
7. Cuffin BN. A method for localizing EEG sources in realistic head model. *IEEE Trans Biomed Eng* 1995; 43: 299-303.
8. He B, Musha T, Okamoto Y, *et al.* Electric dipole tracing in the brain by means of the boundary element method and its accuracy. *IEEE Trans Biomed Eng* 1987; 34:406-14.
9. Wood CC. Application of dipole localization methods to source identification of human evoked potentials. *Ann NY Acad Sci* 1982; 388:139-55.
10. Ebersole JS, Wade PB. Spike voltage topography and equivalent dipole localization in complex partial epilepsy. *Brain Topogr* 1990; 3:21-34.
11. Merlet I, Gotman J. Reliability of dipole models of epileptic spikes. *Clin Neurophysiol* 1999; 110:1013-28.
12. Oliva M, Meckes-Ferbera S, Roten A, Desmond P, Hicks RJ, O'Brien TJ. EEG dipole source localization of interictal spikes in non-lesional TLE with and without hippocampal sclerosis. *Epilepsy Res* 2010; 92:183-90.
13. Meckes-Ferber S, Roten A, Kilpatrick C, O'Brien TJ. EEG dipole source localization of interictal spikes acquired during routine clinical video-EEG monitoring. *Clin Neurophysiol* 2004; 115:2738-43.
14. Plummer C, Litewka L, Farish S, Harvey AS, Cook MJ. Clinical utility of current-generation dipole modelling of scalp EEG. *Clin Neurophysiol* 2007; 118:2344-61.
15. Ebersole JS. Noninvasive localization of epileptogenic foci by EEG source modeling. *Epilepsia* 2000; 41:24-33.
16. Ebersole JS, Wade PB. Spike voltage topography identifies two types of frontotemporal epileptic foci. *Neurology* 1991; 41:1425-33.
17. Gavaret M, Badier JM, Marquis P, Bartolomei F, Chauvel P. Electric source imaging in temporal lobe epilepsy. *J Clin Neurophysiol* 2004; 21:267-82.
18. Boon P, D'Have M. Interictal and ictal dipole modeling in patients with refractory partial epilepsy. *Acta Neurol Scand* 1995; 92:7-18.
19. Boon P, D'Have M, Adam C, *et al.* Dipole modeling in epilepsy surgery candidates. *Epilepsia* 1997; 38:208-18.
20. Boon P, D'Have M, Van Hoey G, *et al.* Interictal and ictal source localization in neocortical versus medial temporal lobe epilepsy. *Adv Neurol* 2000; 84:365-75.
21. Lantz G, Ryding E, Rosen I. Three-dimensional localization of interictal epileptiform activity with dipole analysis: comparison with intracranial recordings and SPECT findings. *J Epilepsy* 1994; 7:117-29.
22. Lantz G, Holub M, Ryding E, Rosen I. Simultaneous intracranial and extracranial recording of Interictal epileptiform activity in patients with drug resistant partial epilepsy: patterns of conduction and results from dipole reconstructions. *Electroencephalogr Clin Neurophysiol* 1996; 99(1):69-78.
23. Lantz G, Ryding E, Rosen I. Dipole reconstruction as a method for identifying patients with mesolimbic epilepsy. *Seizure* 1997; 6:303-10.
24. Foldvary N, Klem G, Hammel J, Bingaman W, Najm I, Luders H. The localizing value of ictal EEG in focal epilepsy. *Neurology* 2001; 57:2022-8.
25. Schneider MR. A multistage process for computing virtual dipolar sources of EEG discharges from surface information. *IEEE Trans Biomed Eng* 1972; 19:1-12.
26. Brody DA, Terry FH, Ideker RE. Eccentric dipole in spherical medium: generalized expression for surface potentials. *IEEE Trans Biomed Eng* 1973; 20:141-3.
27. Kavanagh RN, Darcey TM, Lehmann D. Evaluation of methods for three dimensional localization of electrical sources in the human brain. *IEEE Trans Biomed Eng* 1978; 25:421-9.
28. Darcey TM, Ary JP, Fender DH. Methods for the localization of electrical sources in the human brain. *Prog Brain Res* 1980; 54:128-34.
29. Bai X, Bin H. On the estimation of the number of dipole sources in EEG source localization. *Clin Neurophysiol* 2005; 116:2037-43.
30. Michel C, Lantz G, Spinelli L, Grave de Peralta R, Landis T, Seeck M. 128 channel EEG source imaging in epilepsy: clinical yield and localization precision. *J Clin Neurophysiol* 2004; 21:71-83.
31. Gavaret M, Badier JM, Marquis P, *et al.* Electric source imaging in frontal lobe epilepsy. *J Clin Neurophysiol* 2006; 4:358-70.
32. Gavaret M, Trébouchon A, Bartolomei F, *et al.* Source localization of scalp-EEG interictal spikes in posterior cortex epilepsies investigated by HR-EEG and SEEG. *Epilepsia* 2009; 50: 276-89.

33. Mine S, Yamaura A, Iwasa H, *et al.* Dipole source localization of ictal epileptiform activity. *Neuroreport* 1998; 9:4007-13.
34. Homma I, Masaoka Y, Hirasawa K, *et al.* Comparison of source localization of Interictal epileptic spike potentials in patients estimated by the dipole tracing method with the focus directly recorded by the depth electrodes. *Neurosci Lett* 2001; 304:1-4.
35. Shindo K, Ikeda A, Musha T, *et al.* Clinical usefulness of the dipole tracing method for localizing interictal spikes in partial epilepsy. *Epilepsia* 1998; 39:371-9.
36. Rojo P, Caicoya AG, Martin-Loeches M, *et al.* Localization of the epileptogenic zone by analysis of electroencephalographic dipole. *Rev Neurol* 2001; 32:315-20.
37. Brodbeck V, Lascano AM, Spinelli L, Seeck M, Michel CM. Accuracy of EEG source imaging of epileptic spikes in patients with large brain lesions. *Clin Neurophysiol* 2005; 116: 2037-43.
38. Krings T, Chiappa KH, Cuffin BN, Cochius JI, Connolly S, Cosgrove GR. Accuracy of EEG dipole source localization using implanted sources in the human brain. *Clin Neurophysiol* 1999; 110:106-14.